Journal of Structural Geology 32 (2010) 1030–1045

Contents lists available at ScienceDirect

Journal of Structural Geology

journal homepage: www.elsevier.com/locate/jsg

Conjugate-shear folding: A model for the relationships between foliations, folds and shear zones

Domingo G.A.M. Aerden [a,*], Mohammad Sayab [b], Mohamed L. Bouybaouene [c]

[a] Instituto Andaluz de Ciencias de la Tierra (CSIC), Dpto. de Geodinámica, Universidad de Granada, C/ Fuentenueva s/n, 18002 Granada, Spain
[b] National Centre of Excellence in Geology, University of Peshawar, Pakistan
[c] Université Mohamed V, Dpt. des Sciences de la Terre, Rabat, Morocco

ARTICLE INFO

Article history:
Received 10 December 2009
Received in revised form
31 May 2010
Accepted 18 June 2010
Available online 26 June 2010

Keywords:
Folding mechanism
Crenulation cleavage
Cleavage fanning
Porphyroblast rotation
Conjugate-shear zones

ABSTRACT

Microstructural mapping of whole thin sections cut from two samples of micaschist containing cm-scale folds plus garnet porphyroblasts has provided new insight in the relationships between folding, shearing and foliation development. The garnets exhibit coherent inclusion-trail patterns that place important constraints on the kinematic development of both samples, which are shown to be representative of coaxial versus non-coaxial deformation in rocks containing a pre-existing schistosity. A comparison of crenulations-cleavages geometries in both samples and a review of the geometry of natural and experimental multilayer folds leads to the conclusion that folding involves conjugate shearing at different scales. At microscopic scales, crenulation cleavages nucleate as conjugate-kink or shear instabilities and develop further as a function of the macroscopic partitioning of deformation. In fold-hinge domains, bulk-coaxial deformation results in equal development of conjugate crenulations that progressively coalescence into symmetrical crenulation patterns so that, macroscopically, parallelism is achieved between foliation, fold–axial planes and long axes of strain ellipses. Fold-limb domains represent a system of conjugate-shear zones where single sets of crenulation instabilities with synthetic shearing component preferentially develop producing oblique relationships between the aforementioned elements. Cleavage fanning is inferred as a direct consequence of this conjugate-shear origin of folds. The model implies that crenulation cleavages and S-C fabrics in shear zones form by analogous processes, in both cases involving a component of shearing along foliation planes. The development of conjugate sets of foliation planes surrounding porphyroblasts during early, relatively coaxial stages of deformation explains continued "gyrostatic" behaviour during more advanced non-coaxial stages, as indicated by consistently oriented inclusion trails in the studied samples.

1. Introduction

Tectonic foliations defined by preferred shape orientations of mineral grains are commonly classified as "continuous" foliations and contrasted with "spaced" foliations, which exhibit a distinct microstructural differentiation between discrete cleavage planes (*septae*) and microlithons (e.g. Passchier and Trouw, 2005). Spaced foliations are typical of polymineralic rocks and include the well-known morphological types of slaty-cleavage, crenulation cleavage and shear-band cleavage. A range of microstructural processes have been recognized as playing a role during cleavage differentiation, including micro-kinking or -folding, dissolution and reprecipitation, recrystallization, intra-crystalline deformation, mimetic growth and shear localization (see Passchier and Trouw, 2005 for a review). However, the precise relationships between these processes are not well understood as counts for the macroscopic relationships between foliations and strain patterns in folds and shear zones. A particularly long standing question concerns the mechanical significance of spaced foliations, either as planes of dissolution and volume loss only, or as micro-shear zones (e.g. Siddans, 1972; Gray and Durney, 1979; Hobbs et al., 1982; Williams, 1990; Stewart, 1997).

In this paper, we address these questions in the light of detailed microstructural mapping of whole thin sections that were cut from two samples of fine-grained micaschist containing cm-scale folds. The kinematic evolution of both samples is uniquely constrained by numerous garnet porphyroblasts, whose inclusion trails exhibit coherent orientation patterns exhibiting particular relationships with the host folds. Symmetrical versus asymmetrical relationships demonstrate bulk-coaxial versus bulk non-coaxial deformation in

* Corresponding author. Tel.: +34 958 242825; fax: +34 958 248527.
E-mail address: aerden@ugr.es (D.G.A.M. Aerden).

0191-8141/$ – see front matter © 2010 Elsevier Ltd. All rights reserved.
doi:10.1016/j.jsg.2010.06.010

the samples, respectively, which was in both cases superposed on pre-existing penetrative schistosity. A comparison of crenulation-cleavage patterns developed in both samples and a review of the geometry and kinematics of experimental or natural multilayer folds leads us to propose a new folding mechanism called "conjugate-shear folding". The model reduces the difference between shear zones and folds to a matter of scale, and has major implications for the mechanical significance of spaced cleavages, the origin of cleavage fanning, porphyroblast rotation and the distinction between genuine and pseudo-S-C fabrics as discussed.

2. Sample -A-

2.1. General description

The first studied sample (sample -A- further) is a fine-grained graphitic micaschist from the Rif mountains in North Morocco. It was collected from a coastal outcrop west of the town of Ceuta in the Palaeozoic Beni-Mzala unit of the Alpujarride–Sebtide complex (Betic-Rif orogen; Fig. 1a). Bouybaouene et al. (1995) determined peak metamorphic conditions of about 12 kbar and 500 °C for this unit. The single thin section studied from this sample was cut perpendicular to cm-scale fold- and crenulation axes (Fig. 2a, b) and exhibits a principle anticline–syncline pair outlined by fine bedding laminae. It contains a total of 65 garnet porphyroblasts with diameters in the range of 0.75–1 mm and relatively even distribution across the fold pair, plus a dozen tiny cloritoid porphyroblasts (diameters < 0.5 mm) that cluster in a restricted area. All porphyroblasts contain straight to weakly crenulated inclusion trails composed of fine-grained graphite, opaque minerals and quartz (Fig. 3a, b). The trails are continuous with the principle matrix schistosity (S_1), which appears strongly overprinted by a well developed crenulation cleavage (S_2) genetically related to the main folds. Two coarse-grained quartz–calcite veins sharply cut S_2, do not show signs of internal deformation and therefore probably post-date folding.

2.2. Inclusion-trail data

Accurate line tracings of all inclusion trails in sample -A- on high-magnification photomicrographs revealed their alignment along weakly undulating surfaces that follow the much tighter fold pattern in the matrix (Figs. 2b and 4). A similar geometric relationship was reported earlier by Visser and Mancktelow (1992) in a garnet bearing, decimetre-scale fold in the Swiss Alps. These authors interpreted that the garnets predated folding but during folding experienced differential rotations in opposite fold-limbs due to a combination of flexural-flow and homogeneous flattening. This model appeared to account for an alleged relationship between inclusion-trail orientation and porphyroblast ellipticity. However, Forde and Bell (1993) and Bell and Forde (1995) contested this relationship and proposed an alternative interpretation. They argued that the porphyroblasts nucleated early during folding and did not experience subsequent rotations relative to the axial plane of the fold (cf. Bell, 1985), so that the garnets would have effectively "fixed" an early fold-development stage.

Which of these interpretations (if either) applie to sample -A-? A first point relevant to this question is that many of the inclusion trails in sample -A- are weakly crenulated, thereby demonstrating that porphyroblasts nucleated early during folding (Figs. 2b and 3a, b). Moreover, measurements for the axial planes of included crenulations (incipient S_2) do not reveal a significant statistical differences between adjacent fold-limb domains, contrary to what is shown by the inclusion trails themselves (S_1; Fig. 4a–c). Although data are admittedly scarce in two of the fold-limb domains, these points tend to support the "fixed-fold" hypothesis. On the other hand, the relatively large spread of crenulation orientations in porphyroblasts is suggestive of differentially rotated porphyroblasts within single fold-limb domain. A possible explanation of this paradox is proposed later in this paper.

2.3. Cleavage fanning

Accurate tracing of S_2 cleavage septae (Fig. 2b) revealed that the changes in orientation of this foliation giving rise to cleavage fanning are not gradual, but produced discontinuously across a number of "unconformities" that separate different S_2-dip domains. Indeed, two sub-sets of S_2 septae can be distinguished dipping in opposite directions with respect to the axial plane of the folds and showing opposite offsets of intersected bedding laminae and S_1 (Fig. 5). In principle, such offsets do not demonstrate shearing along foliation planes as they can, alternatively, be interpreted as geometric effects of dissolution and volume loss concentrated in crenulation-limb domains. However, in sample -A-

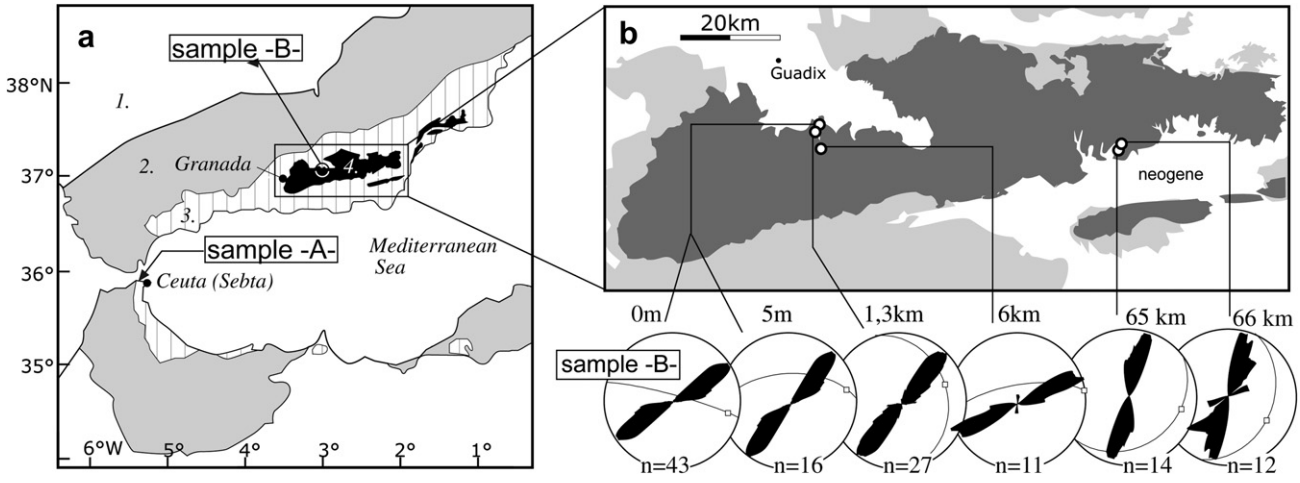

Fig. 1. (a) Overview map of the Betic-Rif orogen showing the locations of samples -A- and -B-. (1): Iberian foreland, (2): Mesozoic-Tertiary sediments, (3): Alpujarride–Sebtide complex, (4): Nevado-Filabride complex. (b) Rose diagrams showing similar strikes of inclusion trails in sample B and five other samples from the Veleta nappe. Note that the orientations of matrix foliation (great circles) and lineation (open squares) in the samples vary considerably.

Fig. 2. (a) Thin section studied of sample -A- oriented normal to fold axes. A higher-resolution image has been placed in the electronic supplement. (b) Microstructural map of (a) showing lithology, S_2 cleavage septae, and S_1 inclusion trails in garnet and some cloritoid porphyroblasts. A synthetic sketch (inset) highlights unconformity-like features associated with divergent fanning of S_2 cleavage.

shearing components along S_2 foliation septae are strongly suggested by the direct relationship between foliation orientation and offset sense, plus the wedge-shaped geometry of individual microlithons and low-strain domains (Figs. 3c and 5) associated with the aforementioned "unconformities". Additional, and perhaps more important components of shortening are implied by selective dissolution of quartz from cleavage planes responsible for their compositional differentiation. Thus, S_2 is best interpreted as a system of conjugate micro-shear zones that accommodated components of shearing, shortening and volume loss. This fabric developed in response to bulk shortening that was initially oriented subparallel to bedding plus S_1 as witnessed by the symmetry of the thin section-scale inclusion-trail pattern with respect to the folds.

3. Sample -B-

3.1. General description

Our second sample (sample -B- further) is also a fine-grained micaschist of Palaeozoic age from the Betic-Rif orogen, but from the lower nappe unit of the Nevado-Filabride Complex (SE Spain; Fig. 1a). According to Booth-Rea et al. (2003), the metamorphic path of this unit (known as the Veleta- or Ragua nappe) was characterized by peak pressure of 12–14 kbar at 320–450 °C followed by extensive metamorphic re-equilibration at 9 kbar and 450 °C. The sample was studied in three extra-large sized (5 × 7 cm) thin sections, two of which are horizontal and the third vertical with N–S strike. These particular orientations were originally chosen for the purpose of a regional-scale correlation of inclusion trails and matrix fabrics presented in Aerden and Sayab (2008). However, in sample -B- these orientations happen to coincide approximately with "L-sections" (normal to foliation and parallel to lineation) and "P-sections" (normal to both foliation and lineation), and hence are also useful for studying the kinematic history of the sample. High-resolution scanned images of all three thin sections plus microphotographs of all porphyroblasts represented in Fig. 6b are provided in an electronic supplement to this article.

All three thin sections are sub-perpendicular to the axial planes of upright, cm-scale folds associated with a penetrative matrix schistosity (S_1) defined by white mica, quartz, opaque minerals and relatively large, partially chloritized biotite laths. The folds are clearly outlined by two subparallel quartz veins that also exhibit parasitic folding and micro-boudinage features (Fig. 6a–d). A well-developed mineral lineation is associated with this fabric and plunges 15° east, slightly shallower than fold (35° east). The folds host numerous garnet porphyroblasts, about double in size as the

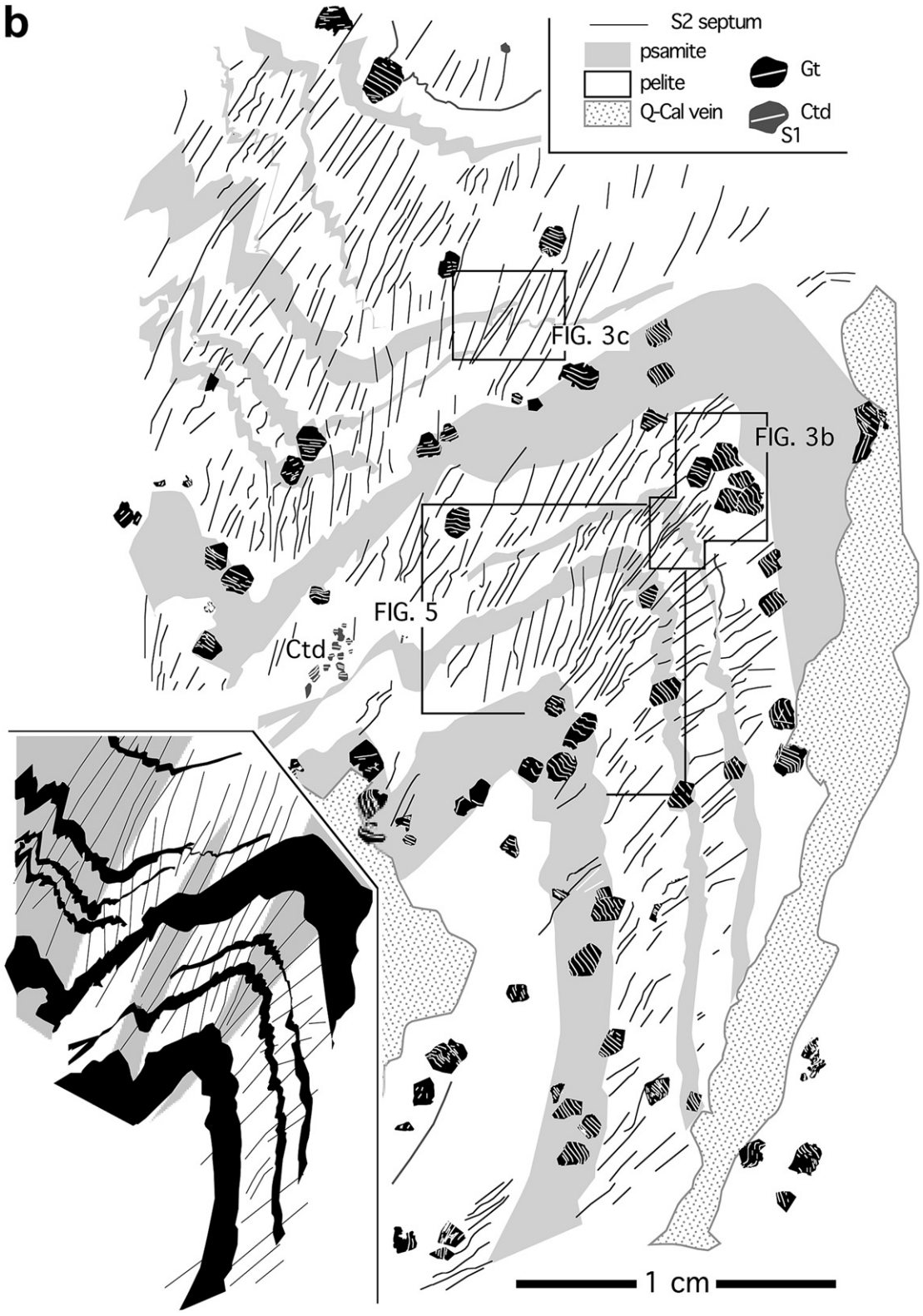

Fig. 2. (*continued*).

garnets in sample -A-, which contain relatively coarse-grained inclusion trails of quartz and opaque minerals. The trails are straight to weakly sigmoidal, continuous with the principle matrix schistosity (S_1) but systematically oriented oblique to this fabric. In other words, the porphyroblasts appear rotated. The average angle between S_1 as defined by inclusion trails and matrix S_1 is 65° in the horizontal section (approximate "L-section"; Fig. 6b).

A second, widely spaced crenulation cleavage (S_2) is also developed in the sample and makes a low angle with S_1 so that both foliations are difficult to distinguish in outcrop. S_2 cleavage planes

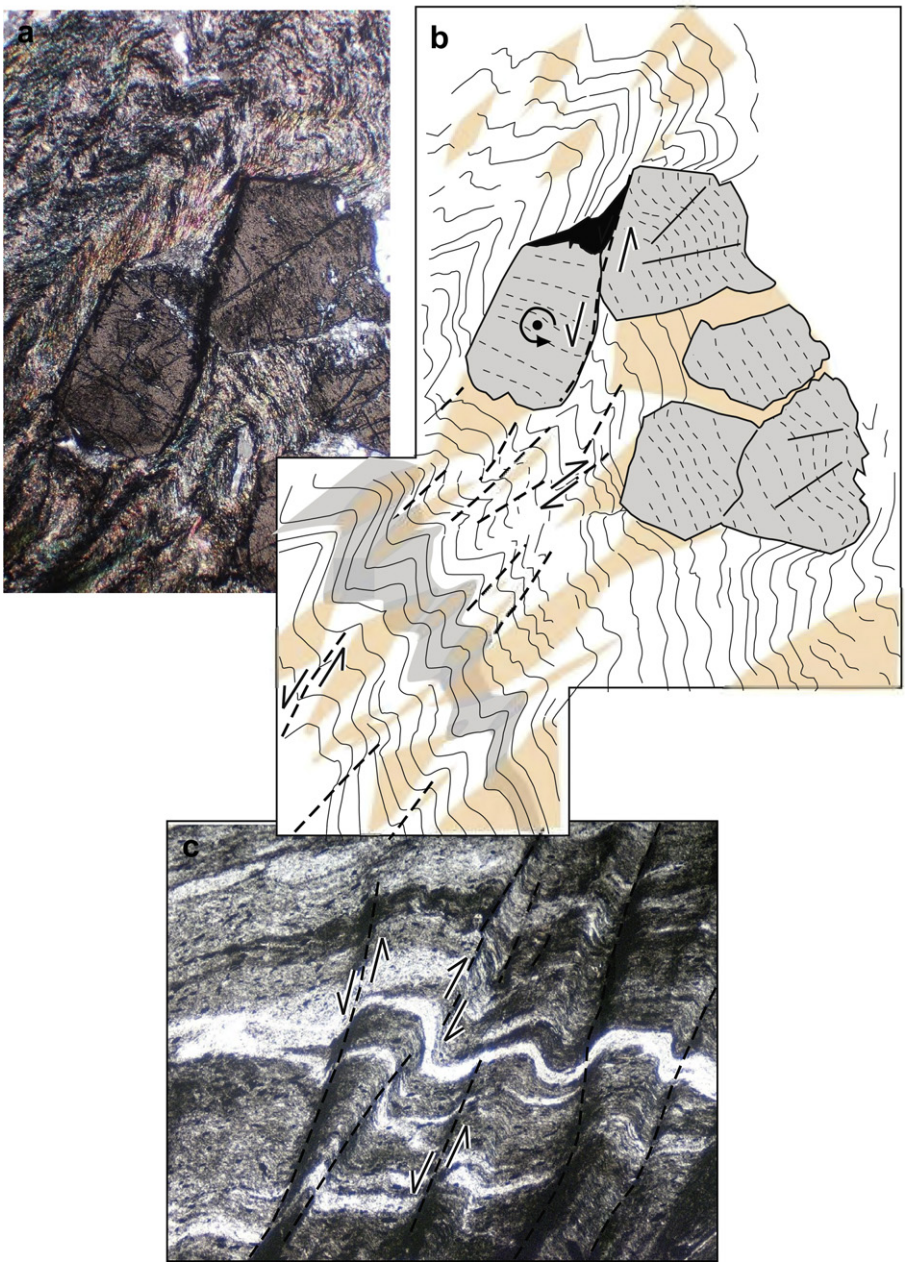

Fig. 3. Close-ups of areas indicated in Fig. 2a. (a) Photomicrograph of the two porphyroblasts on the left in (b). (b) Accurate line tracing of matrix crenulations and inclusion trails. Note conjugate-crenulation geometry within two porphyroblasts. Bold stipple lines indicate compositionally differentiated S_2 septae. The left-most porphyroblast appears to have rotated relative to the rest due to matrix-porphyroblast detachment and pressure-fringe growth (solid black). Lozenge-shaped crenulation-hinge domains (light-orange) conserve the original orientation of S_1 and resemble similar elements in multilayer folds in Fig. 8. (c) Wedge-shaped microlithon bound by S_2 septae indicative of (conjugate) shearing components along cleavage septae. (For interpretation of the references to colour in this figure legend, the reader is referred to the web version of this article.)

are associated with sigmoidal ("extensional") crenulations of S_1 and produce thinning and asymmetric boudinage of the quartz veins where they cut across them (Fig. 6b, c). The asymmetry of these microstructures as seen in the horizontal thin section, subparallel to the mineral lineation, indicates a component of dextral shearing parallel to S_2.

3.2. Inclusion-trail data

Orientation measurements for the inclusion trails in sample -B- reveal a high degree of consistency both in the horizontal and vertical section. A stereoplot containing this data is shown in Fig. 6e and reveals the 3-D preferred orientation of these microstructures according to a steeply SE dipping plane that makes an angle of 65° with S_1 in the matrix. The intersection line between both planes, and hence axes of relative porphyroblast–matrix rotation, plunges 45° east, slightly steeper than the fold axes. Two conflicting interpretations of "rotated" inclusion trails have been debated during the past two decades that can both be considered as potential explanations for the above-described data.

Traditionally, it is assumed that non-coaxial deformation induces porphyroblast rotation due to viscous drag along porphyroblast margins. When applied to sample -B-, this model implies sinistral shearing parallel to S_1 (viewing downwards), which had to be quite homogeneous as all porphyroblasts show similar rotation angles. Homogeneous shearing parallel to S_1 would

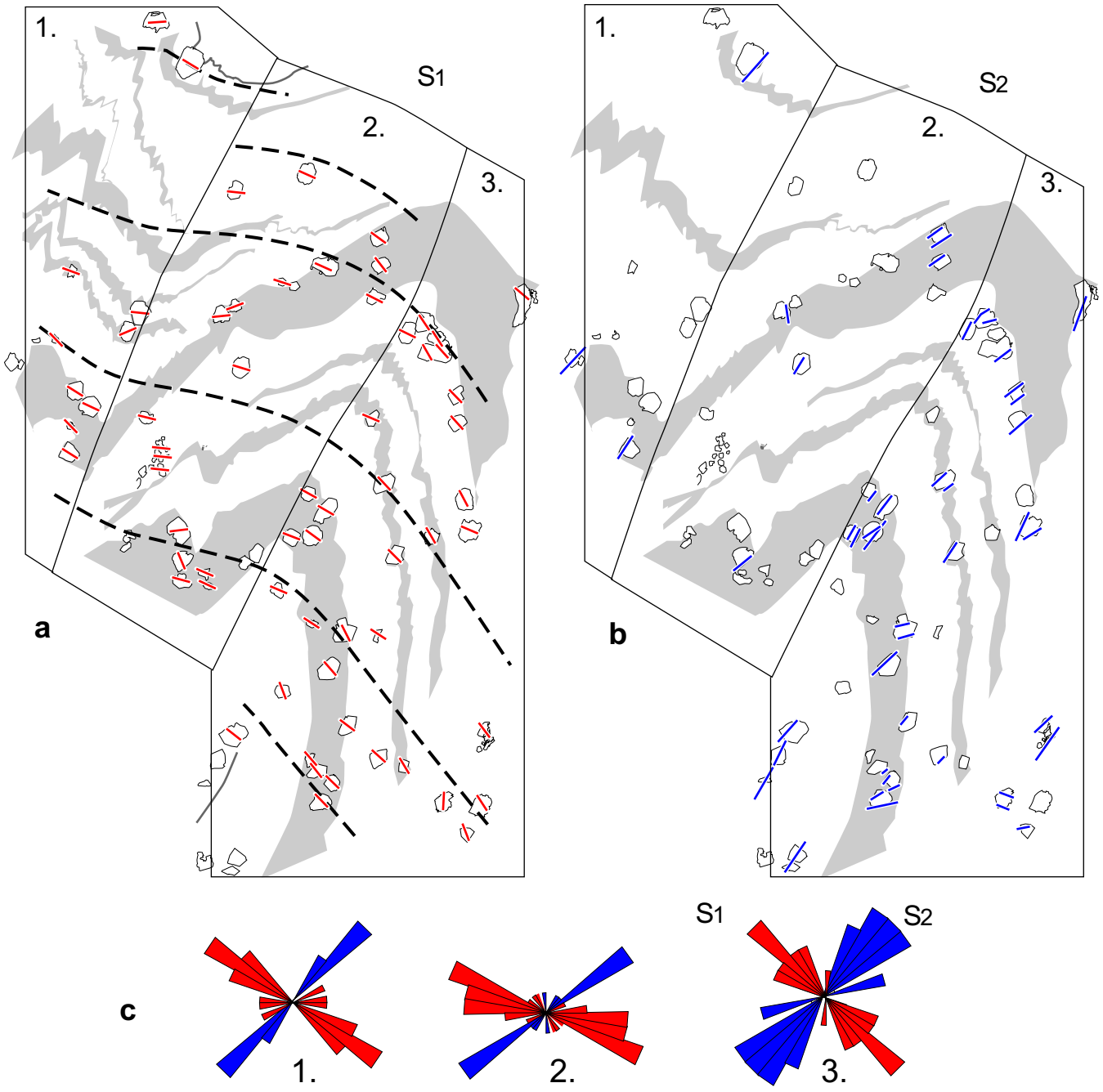

Fig. 4. Higher-magnification microstructural map of area indicated in Fig. 2a. S_2 cleavage septae producing sinistral versus dextral displacements of S_1 are coloured blue and red, respectively. Black lines represent axial planes of symmetrical crenulations in the hinge zone. Note wedge-shaped microlithons confined between converging sinistral and dextral septae. Also note "extensional" crenulation geometries in fold-limb domains.

not have produced tight folds with S_1 as axial plane so these folds had to develop earlier. Indeed, post-folding reactivation of S_1 as a plane of mechanical anisotropy during D_2 deformation is quite plausible, because reactivation shearing is generally antithetic with respect to the bulk shear sense (cf. Aerden, 1995) so sinistral shearing parallel to S_1 is consistent with the earlier concluded dextral shearing parallel to S_2 (synthetic).

The alternative interpretation is that porphyroblasts did not rotate due to intense partitioning of shear-strain components around them causing them to be effectively decoupled from the bulk flow (cf. Bell, 1985; Aerden, 1995; Fay et al., 2009). According to this model, the 65° angle between inclusion trails and S_1 in sample -B- corresponds to progressive reorientation of S_1 in the D_2 flow relative to porphyroblasts that maintained stable orientations. We prefer this second interpretation because of the following considerations.

Firstly, the sigmoidal geometry of S_1 preserved within porphyroblasts plus immediately adjacent strain-shadow regions mimics that of F_2 matrix crenulations elsewhere in the matrix and sigmoidal vein segments bound by S_2 planes. These microstructures consistently record a clockwise reorientation of S_1 from zones of low or zero strain into bounding S_2 cleavage septae, exactly as predicted by the aforementioned partitioning of deformation around rigid objects. If porphyroblasts had rotated due to shearing

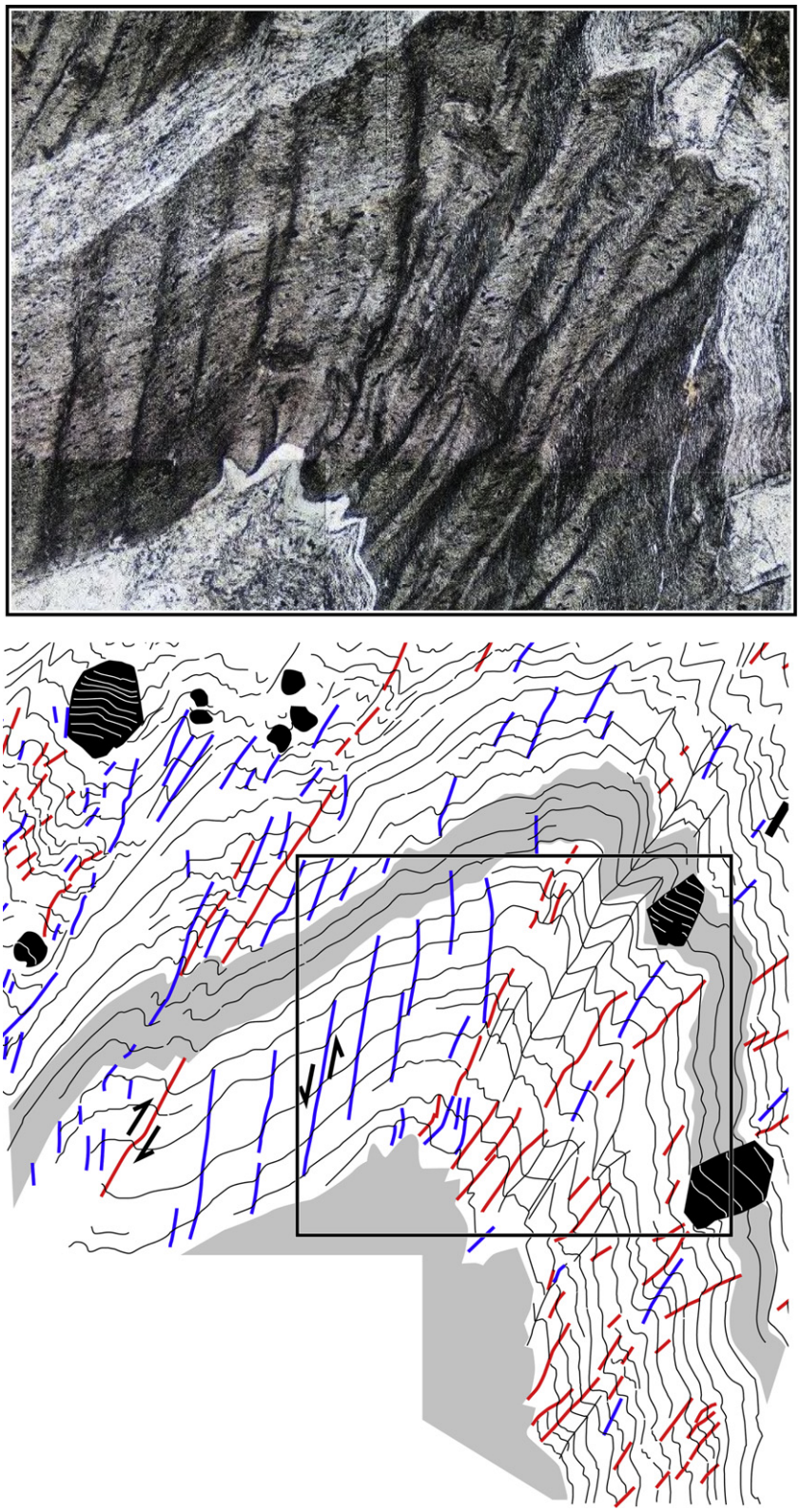

Fig. 5. Higher-magnification microstructural map of area indicated in Fig. 2a. S_2 cleavage septae producing sinistral versus dextral displacements of S_1 are coloured blue and red, respectively. Black lines represent axial planes of symmetrical crenulations in the hinge zone. Note wedge-shaped microlithons confined between converging sinistral and dextral septae. Also note "extensional" crenulation geometries in fold-limb domains.

parallel to S_1 any localization of strain would be expected to have occurred in planes parallel to S_1, not S_2.

Secondly, axes of relative porphyroblast–matrix rotation in sample -B- make an angle of about 30° with a pronounced mineral lineation in the sample and rest of the outcrop from where it was taken. However, if the porphyroblasts were rotated due to shearing parallel to S_1, their rotation axes would be expected to be perpendicular to the mineral lineation, which is not the case. According to the “non-rotation”

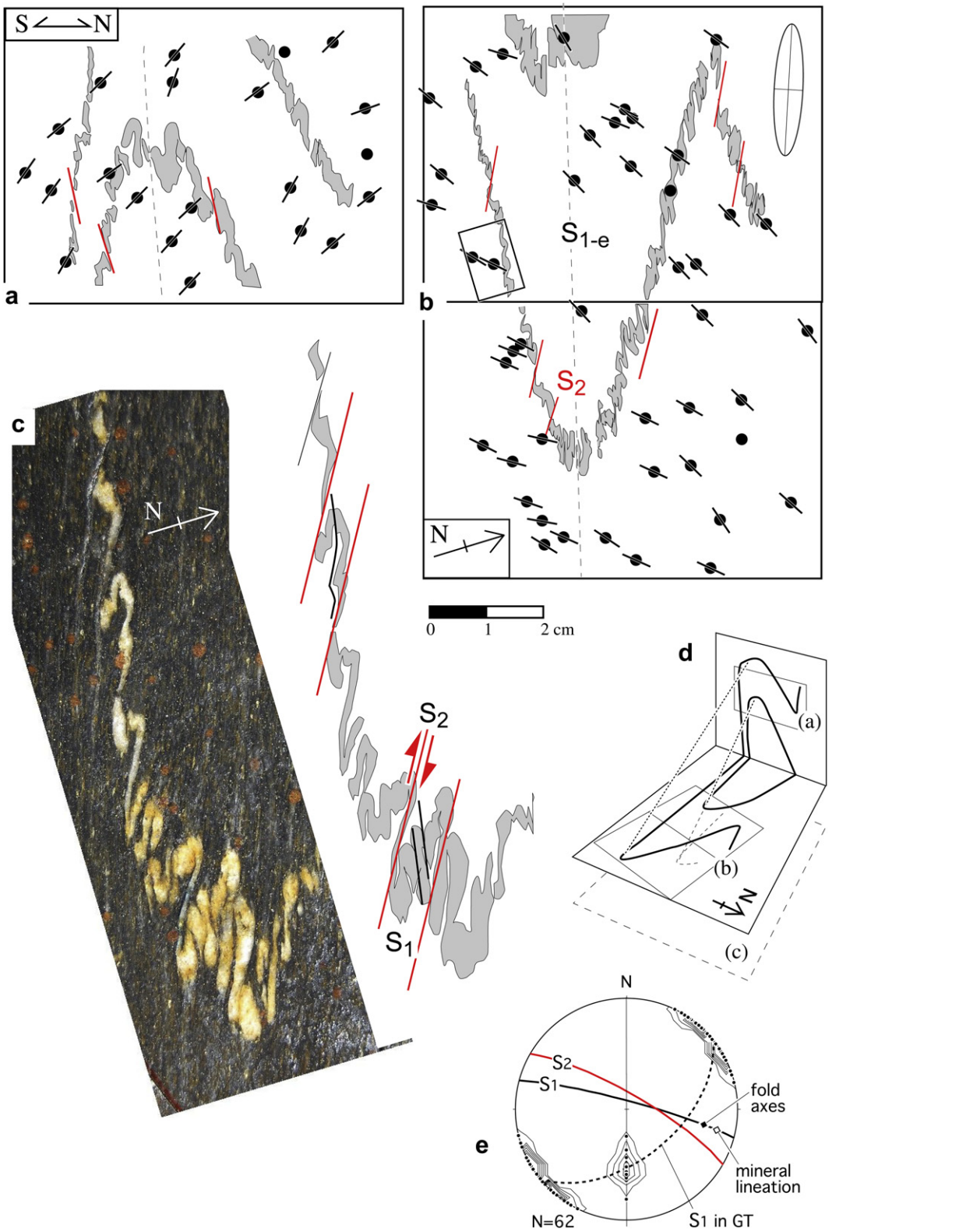

Fig. 6. Microstructural cross-section (a) and map (b) of sample -B- containing folded quartz veins and garnet porphyroblasts whose inclusion-trail orientation have been marked with bars through infilled circles. Strain ellipse in (b) has been copied from Fig. 7b. (c) Horizontal slab showing dextral shearing components parallel to S_2 and its effect on pre-existing F1 parasitic folds. (d) Block diagram showing the spatial relationships between (a), (b) and (c). (e) Stereoplot of S_1 inclusion-trail data (dots) and best-fit plane (stipple line) calculated with FitPitch (Aerden, 2003). The axes of relative porphyroblast-matrix rotation axes plunges 45° East slightly steeper than fold axes and mineral lineation.

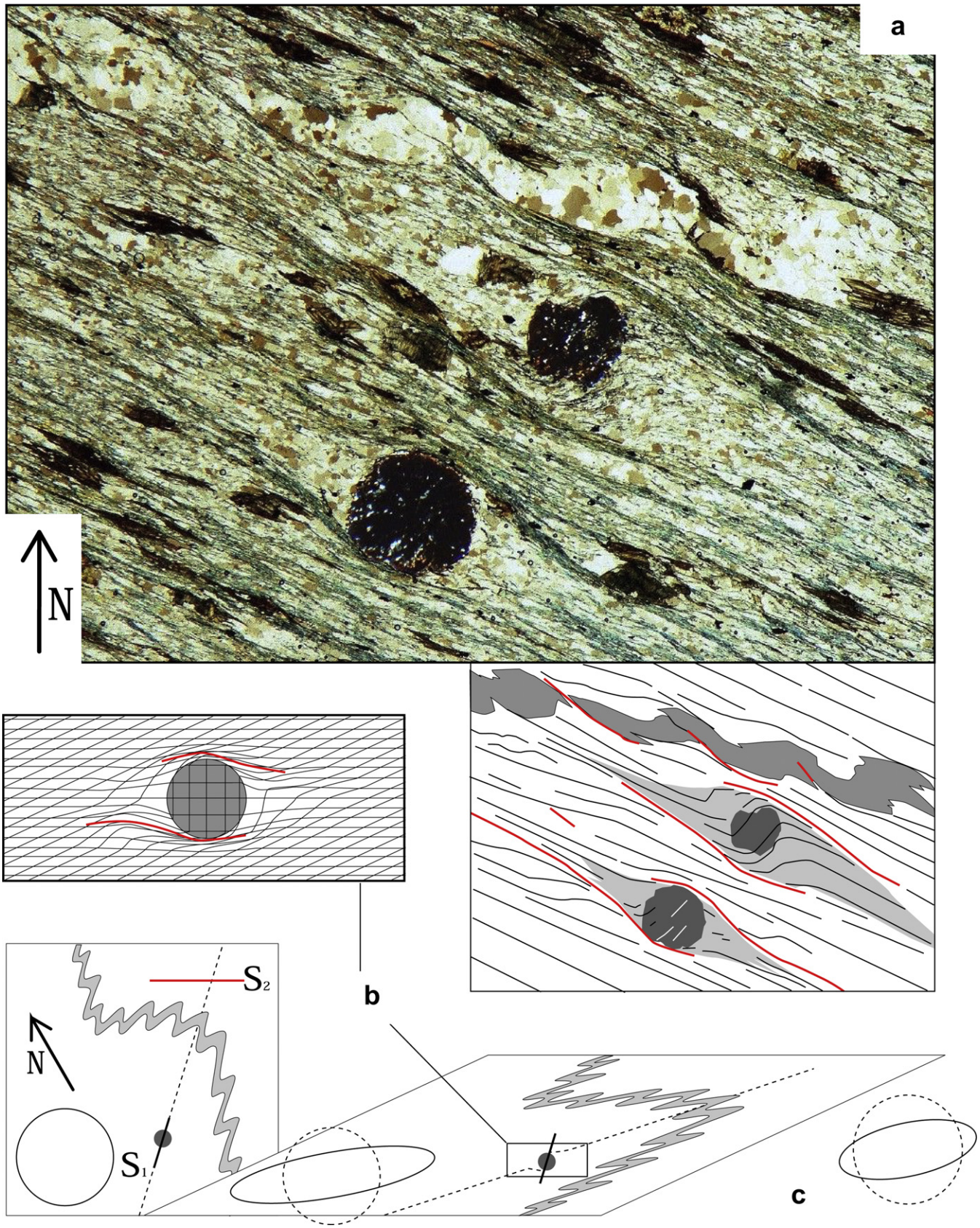

Fig. 7. (a) Microphotograph and accompanying line diagram of area marked in Fig. 6b. Sigmoidal geometries of S_1 within porphyroblasts and adjacent strain shadows, mimic sigmoidal quartz-vein segments bound by S_2 cleavage planes that witness a component of dextral shearing parallel to S_2. (b) Reconstruction of the pre-D2 geometry of the folded vein set in Fig. 6b based on a Mohr diagram construction in which original fold-limb orientations were fitted to the known original orientations of S_1 and S_2. Ellipse axes ratio (Rf) = 4.6; Wk = 0.76. (c) Alternative strain ellipse constructed by Chris Talbot based on his identification of vein segments that were shortened, extended or first shortened then extended during D2 (Rf = 2.9; Wk = 0.21). See text for explanation.

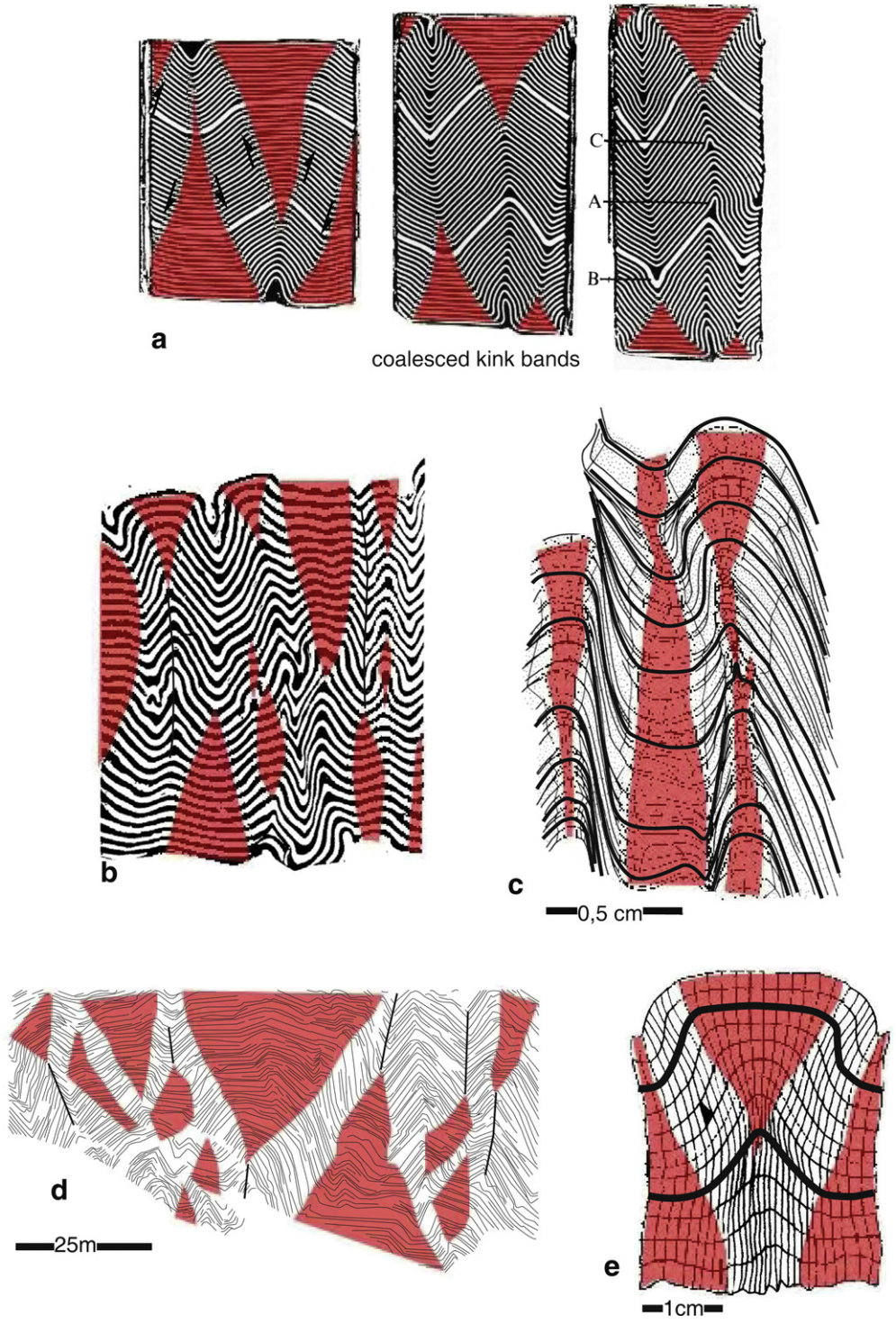

Fig. 8. (a, b) Deformation experimental with plasticine layers described in Price and Cosgrove (1991). Progressive coalescence of conjugate-mechanical instabilities produces chevron-type kinks. Note triangular and lozenge-shaped low-strain domains which preserve the original orientation of the layering. (c) Drawing from Ramsay (1967) of a "similar" fold whose isogons define low-strain zones comparable to the ones shown in (a) and (b). (d) Line drawing after outcrop photograph in Stewart and Alvarez (1991) of kink-style folds in containing lozenge-shaped low-strain domains. (e) Experimental fold produced in salt–mica mixture by Hobbs et al. (1982) illustrating the shear-zone character of fold-limb domains.

interpretation, though, the orientation of relative porphyroblast–matrix rotation axes corresponds to the intersection line between two foliations (S_1 and S_2) that could have any orientation between parallel and perpendicular to kinematic axes.

A third indirect argument supporting "gyrostatic" (Fay et al., 2009) behaviour of porphyroblasts in the Veleta nappe arises from a comparison of the strikes of inclusion trails in sample -B- and in five other samples from the same unit studied by Aerden and Sayab (2008; Fig. 1c). The remarkable consistency of this data would implies unrealistically homogeneous shear strain in the Veleta nappe if porphyroblast rotation is assumed, contradicted by quite variably oriented matrix fabrics of the samples.

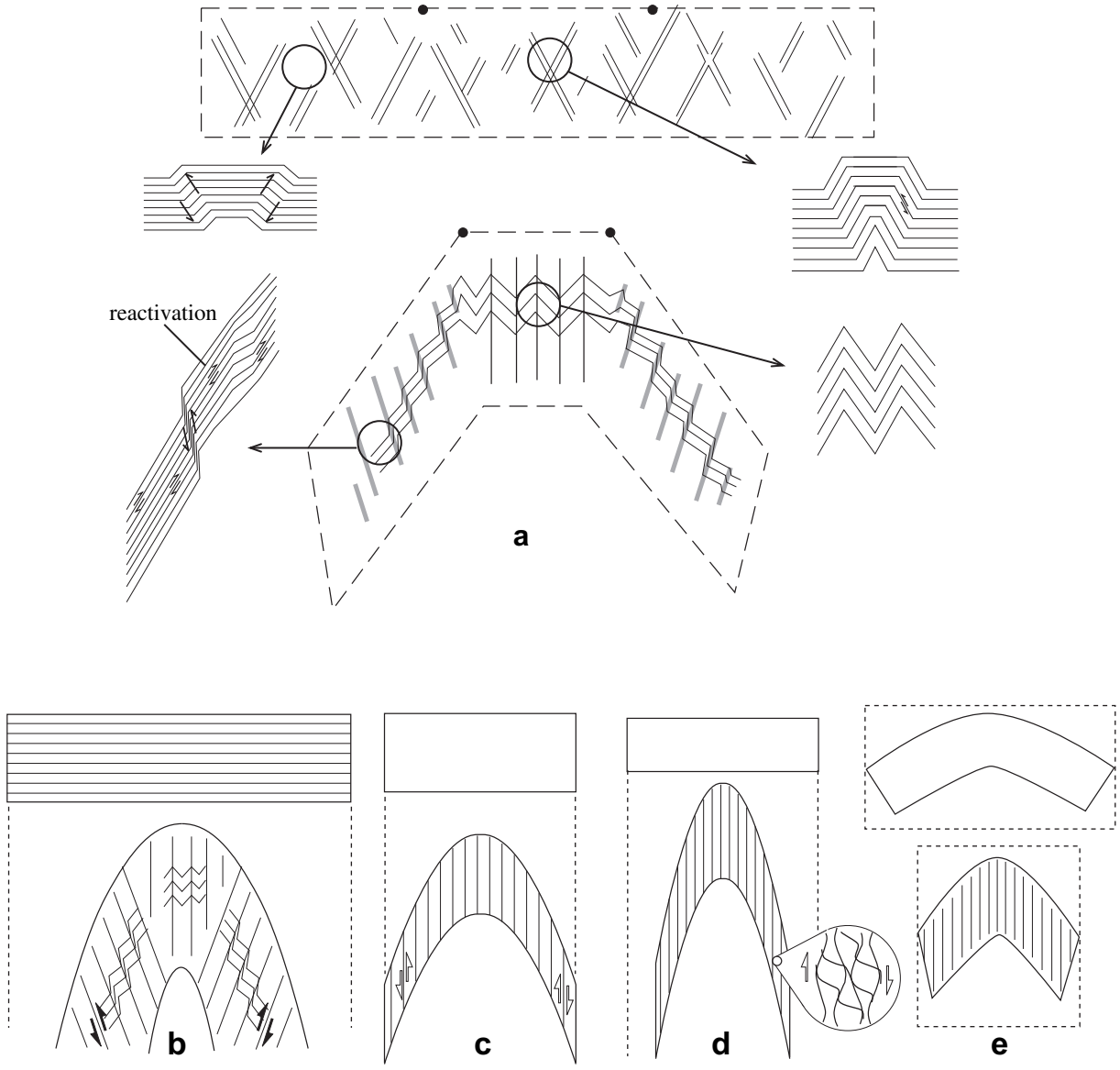

Fig. 9. (a) Conceptual model of spaced foliations forming during layer-parallel shortening. In hinge domains, conjugate crenulations evolve towards symmetrical crenulations. In fold-limb domains, crenulation bands with synthetic shearing components develop preferentially and become compositionally differentiated due to dissolution and volume loss. Antithetic crenulations are destroyed by antithetic reactivation of the anisotropy. (b-e) Comparison of different mechanisms of folding and associated foliation development: (b) conjugate-shear folding (this paper), (c) heterogeneous simple shear, (d) heterogeneous bulk shortening (Bell, 1981), (e) buckling followed by pure shear. Shearing along vertical foliation planes in (c) and (d) is mechanically impossible because there are no resolved shear stresses in this plane.

Considering these three points, our kinematic interpretation of sample -B- envisages a first deformation (D_1) that caused shortening and folding of a set of quartz veins. A second non-coaxial deformation (D_2) subsequently reoriented the axial plane of the folds by 65° but not the porphyroblasts. Porphyroblasts probably nucleated early during D_2, which explains the minor but systematic variations in strike exhibited by inclusion trails in different areas of the thin sections (Fig. 6a, b) in a similar way as argued for the weak folds fixed in the garnets of sample -A-.

3.3. Reconstruction of a strain ellipse

Preservation of the original orientation of S_1 in porphyroblasts provides an opportunity to reconstruct a strain ellipse for D_2 deformation in sample -B-, assuming that S_2 represents the flow plane. We only present the results of a 2-D analysis for Fig. 6b based on a Mohr-diagram construction for the Lagrangian displacement gradient tensor "F" (Means, 1982), in which polar coordinates give the amount of rotation and stretch of material lines as a function of their (original) angles in the undeformed state. The original angles of F_1 fold-limbs (Fig. 7b) were fitted in this diagram to the known original angles of flow plane (S_2) and axial plane of the fold (S_1). The construction is given as an electronic supplement to this article.

Interestingly, Chris Talbot who acted as a reviewer of this paper, performed an alternative strain-analysis of Fig. 6b based on his identification of vein segments that were extended, shortened, or shortened then extended during D_2, and subsequently applying the technique of Passchier (1990 - his Fig. 9). Although somewhat subjective due to the need to distinguish between the effects of D_1 and D_2 on the finite vein geometry, the strain ellipse obtained with this method (Fig. 7c) has similar shape and orientation as the one we determined and confirms a dextral general-flow regime during D_2. Additionally, an area reduction of 36% is suggested, due to extension in the third dimension (Y) plus some volume loss.

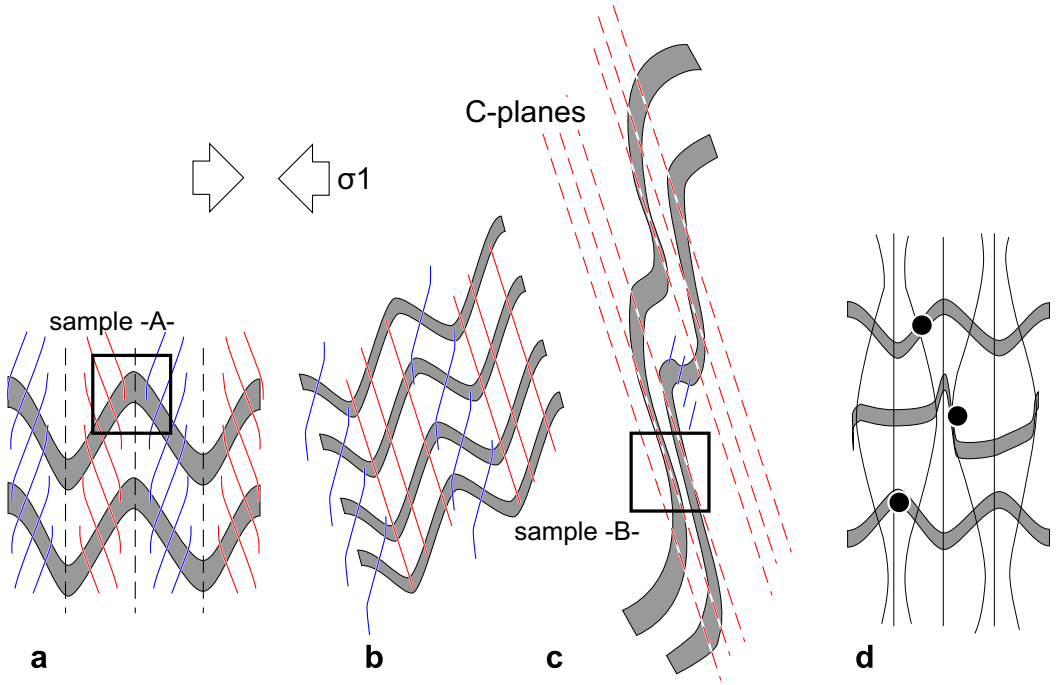

Fig. 10. Conceptual geometric relationships between foliations in (a) symmetric folds, (b) asymmetric folds, and (c) shear zones as a function of increasing non-coaxiality of deformation. Arrows indicate maximum stress direction. (d) Possible large-scale context of (a), (b) and (c).

4. Conjugate-shear folding

In retrospect, the principle differences between samples -A- and -B- as described in the previous sections can be summarized as: (1) the syn-folding versus post-folding timing of porphyroblasts, respectively, and (2) bulk-coaxial versus non-coaxial deformation in both cases superposed on a pre-existing schistosity. We will now compare our kinematic interpretations of both samples with the kinematics of multilayer folds in general as can be directly observed in experiments, or inferred indirectly from the geometry of natural examples.

Experimental folding of multilayers, generally, commences with the development of conjugate-shear instabilities, which, depending on the scale and degree of mechanical anisotropy (controlled by layers thickness, viscosity contrasts, foliations etc.) can take the form of sharp kink-bands, smoother buckle/crenulation bands or narrow shear bands (Fig. 8a, b). Continued deformation causes conjugate-kink or buckle-bands to progressively coalesce into symmetrical chevron-type fold patterns whose axial planes are oriented normal to the shortening direction (Paterson and Weiss, 1966; Cosgrove, 1976; Hobbs et al., 1982; Price and Cosgrove, 1991; Stewart and Alvarez, 1991; Fowler and Winsor, 1996; Fig. 8a, b). This coalescence process involves progressive migration of fold-hinges, and when it does not reach completion leaves characteristic elliptical- to lozenge-shaped low-strain domains (i.e. fold-hinges) surrounded by a system of conjugate-shear zones represented by fold-limb domains (Fig. 8a, b, e). Similar geometries can be readily recognized in natural multilayer folds of quite different styles as is illustrated in Fig. 8c and d, suggesting that the coalescence mechanism operates under a wide range of metamorphic conditions (Stewart and Alvarez, 1991; Fowler and Winsor, 1996).

Symmetrical crenulation patterns in hinge domains of sample -A- are also characterized by isolated, lozenge-shaped low-strain elements which we infer to have formed by progressive coalescence of initial conjugate crenulations (Figs. 3a, b and 5). Such a model is supported by conjugate-kink geometries preserved in some of the porphyroblasts (Fig. 3a, b), and agrees well with the conclusions of earlier works regarding the conjugate nature of incipient crenulation cleavage (e.g. Cosgrove, 1976; Beaumont-Smith, 2001). Significantly, conjugate orientations of S_2 included in porphyroblasts of sample -A- (see Section 2.2) may explain the ca. 45° spread of S_2 in Fig. 4b, but no statistical difference between adjacent fold-limb domains. However, limited differential porphyroblast rotations resulting from local matrix–porphyroblast detachment as suggested, for example, in Fig. 3b would have further contributed to this spread (cf. Aerden, 1996).

Fold-limb domains in sample -A- are characterized by fully differentiated cleavage septae due to the effects of quartz dissolution and mica enrichment. We suggest that these cleavage septae evolved from initial kink-instabilities with synthetic shear component relative to fold-limb rotation as shown conceptually in Fig. 9a. Selective dissolution of quartz in progressively developing kink/crenulation bands can be attributed to a combination of factors, including enhanced micro-permeability associated with grain-boundary sliding parallel to S_1, increased elastic strain of mineral grains, and/or increased crystal plastic deformation resulting in higher dislocation densities and hence solubility. Thus, according to our model, dissolution was strain-induced (cf. Bell and Cuff, 1989) and only indirectly controlled by the orientation of stresses.

5. Discussion

5.1. Comparison with earlier fold- and foliation models

The above proposed conjugate-shear folding model coincides with other folding mechanisms that attribute shearing components to foliations (De Sitter, 1956; Bell, 1981, 1985; Williams, 1990; Fig. 9c, d) as opposed to models that assume shortening and volume loss only (e.g. Gray and Durney, 1979; Fig. 6e). However, our model solves the mechanical problem of shearing in a plane oriented perpendicular to the bulk-shortening direction which lacks resolved shear stresses. Assuming an anastomosing geometry

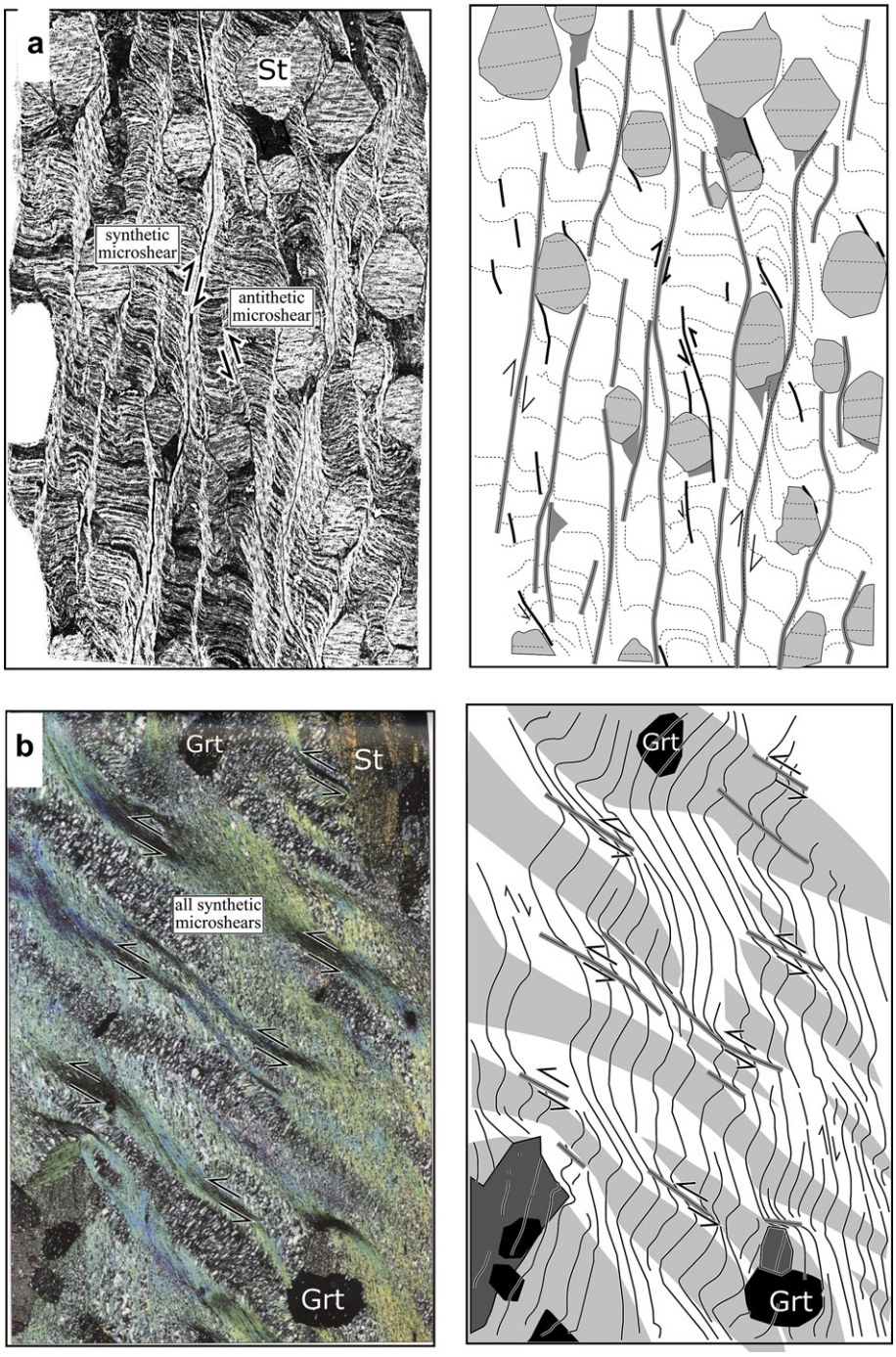

Fig. 11. (a). Example of asymmetric crenulation cleavage in staurolite schist modified after Bell and Cuff (1989) and interpretative sketch. Anastomosing geometries result from the interference of two sets of cleavage planes with synthetic (grey lines) and antithetic (black lines) shearing components. (b) Example of asymmetric crenulation cleavage shown in Vernon (2000), reproduced with permission of Cambridge University Press, and interpretative sketch. Its anastomosing character results from variable widths of short-limb (grey) and long-limb domains, possibly influenced by the presence of rigid porphyroblasts. Yet, fully differentiated S_2 cleavage septae (dark lines) are still subparallel and are interpreted as a single set of synthetic shear bands with shortening components.

of foliation planes (Bell, 1981, 1985; Fig. 9d) does not solve this problem as long as the average orientation remains is still perpendicular to the bulk-shortening direction (cf. Kraus and Williams, 1998). In our model (Fig. 9a, b), foliations form oblique to the bulk-shortening direction, although at relatively high (>45°) angles which may be further increased during progressive fold tightening.

Fig. 10 sketches the conceptual relationships envisaged by our model between simultaneously developing folds, shear zones and their respective fabrics as a function of the same stress field. The model matches reported field relationships between simultaneously developed folds and shear zones, notably as described by Carreras et al., (2005), and presents close analogies with conceptual models of anastomosing conjugate shear zones accommodating bulk-coaxial deformation (Bell, 1981; Hudleston, 1999). In non-coaxially deforming volumes of rocks, though, our model does not predict anastomosing geometries but rather a single set of subparallel foliation planes with consistent shear sense (Fig. 10c). This prediction conflicts with a universally anastomosing geometry of crenulation cleavage assumed in Bell (1985 – his Fig. 1; Fig. 9d) in both coaxially-

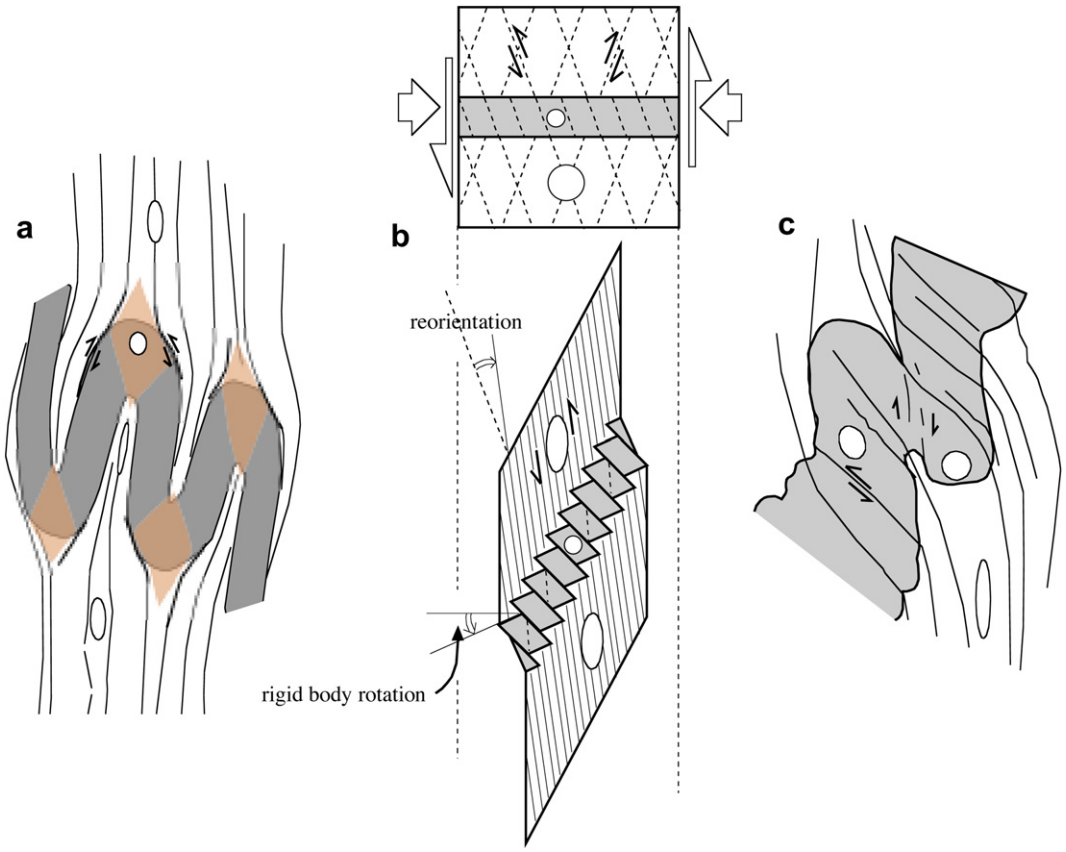

Fig. 12. (a) Line drawing modified after Ramsay and Huber (1987) showing convergent cleavage fanning due to a strong competency contrast between an isolated layers and its matrix. Coloured lozenges represent zones of inferred low-strain. (b) Conceptual model for cleavage refraction. Strain incompatibility between layers with contrasting competencies are solved by rigid-body rotations of more competent microlithons (assumed totally rigid for simplicity). (c) Line drawing after photograph in Tobisch and Paterson (1988) demonstrating the conjugate character of foliation planes refracting through a more competent layer plus inferred (totally hypothetical) strain ellipses.

and non-coaxially deforming rocks. After examining numerous examples of asymmetric crenulation cleavage in thin section and in the literature, we conclude that Bell's (1985; his Fig. 1b) extrapolation to non-coaxial settings of Bell's (1981) "bulk inhomogeneous shortening" model (bulk-coaxial) is insufficiently supported by data. Two examples are presented to illustrate this point.

Fig. 11a (after Bell and Cuff, 1989) shows an apparently anastomosing, asymmetric crenulation cleavage whose asymmetry records a component of dextral shearing. On close examination, however, the anastomosing features in this Figure can be related to two conjugate sets of foliation planes having opposite shear senses, although one of them is dominantly developed. A second example (Fig. 11b; after Vernon, 2000) shows asymmetric crenulation cleavage in which anastomosing geometries result from variable widths of crenulation short-limb and long-limb domains, possibly influenced by presence of large porphyroblasts inside or just outside the plane of the thin section. However, when attention is focused on discrete, fully differentiated cleavage planes in the image, it can be seen that these are all subparallel as the model of Fig. 11 predicts.

5.2. Origin of cleavage fanning and cleavage refraction

Although divergent cleavage fans clearly fit the proposed conjugate-shear folding mechanism, cleavage fanning is not always well developed in folds and some folds show inverse (convergent) cleavage fanning. What controls these variable geometries of foliations in fold? We suggest that limited ($<20^\circ$) cleavage fanning reflects relatively homogeneous deformation with shortening components outweighing the shearing components also in fold-limbs. The lack of appreciable cleavage fanning in sample -B-, however, may be simply due to the composite character of the macroscopic cleavage that intermixes S_1 and S_2. Also, any initial fanning of S_1 would have been significantly reduced during D_2 shearing.

The less common convergent cleavage fans can be attributed to strong competency contrasts between isolated folded layers and their matrix causing the foliation to deflect around low-strain fold-hinges as illustrated in Fig. 12a. Similarly, cleavage refraction can in the context of our model be envisioned as a way of solving strain-incompatibility between layers with different competencies and cleavage spacing (Fig. 12b, c.).

5.3. Foliation development in folds versus shear zones

Criteria for distinguishing "normal" crenulation cleavage formed by polyphase deformation from shear-band cleavages or S-C fabrics produced during a single shearing event are rather ambiguous in the absence of detailed knowledge of the original orientation in which fabrics formed and stress axes (e.g. Passchier and Trouw, 2005; p 130). The recognition of compressional versus extensional (sigmoidal) geometries of crenulations is not conclusive as again illustrated in or samples. In sample -B-, crenulations consistently have extensional geometries because of relatively homogeneous, non-coaxial deformation that caused bulk reorientation and extension of S_1. However, the fabric still formed via two phases of

deformation and in that sense is a normal (polyphase) crenulation cleavage. In sample -A-, similar extensional crenulations are developed in fold-limb domains (Fig. 5), but coexist with "compressional" crenulations in adjacent fold-hinge regions where deformation was coaxial.

In relatively isotropic rocks such as granite, non-coaxial deformation is known to produce S-C fabrics by simultaneous development of a spaced foliation (the "C"-planes) subparallel to shear zones walls, and an oblique "continuous" foliation defined by the shape orientation of initially equigranular or randomly oriented minerals (the "S"-planes). A similar process is highly unlikely, though, in strongly anisotropic, schistose rocks where anisotropy-induced shearing or "reactivation" will prevent the development of a new shape fabric. In other words, only the "C"-planes will materialize, while "S"-planes are inherited from the pre-existing anisotropy. We therefore contend that many, if not all, "S-C resembling structures" developed in slates or micaschists are pseudo-S-C fabrics composed of two superposed foliations lying at a low angle to each other (cf. Aerden, 1998; Aerden and Malavieille, 1999; Aerden and Sayab, 2008; Sayab, 2009). The distinction of genuine versus pseudo-S-C structures, although not critical for correctly determining shear sense, is important as it implies a single phase of deformation versus a polyphase history, respectively.

5.4. Porphyroblast rotation

Inclusion-trail orientation data collected since about 1990 in orogens around the world have increasingly led to the recognition that porphyroblast rotation can be significantly subdued in metamorphic rocks due to deformation partitioning effects related to foliation development processes (e.g. Bell, 1985; Johnson, 1990; Hayward, 1992; Aerden, 1995, 2004; Bell and Forde, 1995; Bell et al., 1999; Jung et al., 1999; Timms, 2003; Sayab, 2005; Evins, 2005; Rich, 2006; Yeh, 2007; Aerden and Sayab, 2008). Yet, lack of porphyroblast rotation during ductile deformation remains a controversial issue, as it does not follow directly from (linear) continuum mechanics, one of the main theoretical pillars on which modelling of "flow in rocks" has been based. Fay et al. (2008, 2009), however, recently presented a numerical simulation that provides a first physical basis for porphyroblast non-rotation. Their modelling highlights the critical role played by conjugate shear bands developing during early coaxial stages of deformation. Continued partitioning of deformation in one set of these bands during subsequent non-coaxial stages of deformation, is what causes "gyrostasis" behaviour of rigid elements. This result is in excellent agreement with our recognition that crenulation cleavages originate as conjugate sets of shear instabilities and the presented evidence for limited or no porphyroblast rotation in two, coaxially- versus non-coaxially deformed samples.

6. Conclusion

Spaced foliations, including crenulation cleavage, shear-band cleavage, but probably also slaty-cleavage at a finer scale, nucleate as conjugate sets of shear- or kink-instabilities that accommodate both pure- and simple-shear components apart from volume loss (dissolution). Equal development and progressive coalescence of both sets in zones undergoing coaxial deformation leads to parallelism between foliations and strain ellipse, whereas in zones of non-coaxial deformation predominant development of one of the sets produces oblique relationships between these elements. The geometry of multilayer folds, including cleavage fanning, reflects a universal mode of deformation partitioning in coaxially deforming fold-hinge domains, and conjugate shearing in fold-limb domains. The same partitioning of deformation at the scale of individual microlithons can be held responsible for stable orientations of rigid objects, even in bulk non-coaxially deforming rocks. The proposed conjugate-shear folding model represents a unified view of folds, shear zones and their respective fabrics. It implies that S-C fabrics and crenulation cleavages originate by similar processes, in all cases involving a component of shearing parallel to cleavage planes.

Acknowledgements

D.A. acknowledges financial support via projects CGL2009-07721 and CSD2006-00041 (Topo-Iberia) from the Spanish Ministry of Science and Innovation, plus project RNM-149 from the Autonomous Government of Andalusia (Junta de Andalucía). We thank Joao Hippertt for editorial handling and Christopher Talbot for a constructive review of an early manuscript. We particularly thank Chris for having drawn our attention to the possibility of strain-analysis in our samples and giving permission to include a result of his own analysis in Fig. 7c.

Appendix. Supplementary data

Supplementary data associated with this article can be found, in the online version, at doi:10.1016/j.jsg.2010.06.010.

References

Aerden, D.G.A.M., 1995. Porphyroblast non-rotation during crustal extension in the Variscan Pyrenees. Journal of Structural Geology 17, 709–726.
Aerden, D.G.A.M., 1996. The pyrite-type strain fringes from Lourdes, France: indicators of Alpine thrust kinematics in the Pyrenees. Journal of Structural Geology 18, 75–92.
Aerden, D.G.A.M., 1998. Tectonic evolution of the Montagne Noire and a possible orogenic model for syn-collisional exhumation of deep rocks, Hercynian belt, France. Tectonics 17, 62–79.
Aerden, D.G.A.M., 2003. Preferred orientation of planar microstructures determined via statistical best-fit of measured intersection-lines: the "FitPitch" computer program. Journal of Structural Geology 25, 923–934.
Aerden, D.G.A.M., 2004. Correlating deformations in the Iberian Massif (Variscan belt) using porphyroblasts; implications for the development of the Ibero-Armorican Arc. Journal of Structural Geology 26, 177–196.
Aerden, D.G.A.M., Malavieille, J., 1999. Origin of a large-scale fold nappe in the Montagne Noire (Variscan Belt, France). Journal of Structural Geology 21, 1321–1333.
Aerden, D., Sayab, M., 2008. From Adria- to Africa-driven orogenesis: evidence from porphyroblasts in the Betic Cordillera, Spain. Journal of Structural Geology 30, 1272–1287.
Beaumont-Smith, C.J., 2001. The role of conjugate crenulation cleavage in the development of 'millipede' microstructures. Journal of Structural Geology 23, 973–978.
Bell, T.H., 1981. Foliation development: the contribution, geometry and significance of progressive bulk inhomogeneous shortening. Tectonophysics 75, 273–296.
Bell, T.H., 1985. Deformation partitioning and porphyroblast rotation in metamorphic rocks: a radical reinterpretation. Journal of Metamorphic Geology 3, 109–118.
Bell, T.H., Cuff, C., 1989. Dissolution, solution transfer, diffusion versus fluid flow and volume loss during deformation/metamorphism. Journal of Metamorphic Geology 7, 425–448.
Bell, T.H., Hickey, K.A., Upton, G.J.G., 1999. Distinguishing and correlating multiple phases of metamorphism across a multiply deformed region using the axes of spiral, staircase, and sigmoidally curved inclusion trails in garnet. Journal of Metamorphic Geology 16, 767–794.
Bell, T.H., Forde, A., 1995. On the significance of foliation patterns preserved around folds by mineral overgrowth. Tectonophysics 246, 171–181.
Booth-Rea, G., Azañon, J.M., Martínez-Martínez, J.M., 2003. Metamorfismo de AP/BT en metapelitas de la unidad de Ragua (complejo Nevado-Filabride, Cordillera Bética). Resultados termo-barométricos del estudio de equilibrios locales. Geogaceta 34, 87–90.
Bouybaouene, M.L., Goffé, B., Michard, A., 1995. High-pressure, low-temperature metamorphism in the Sebtides nappes, northern Rif, Morocco. Geogaceta 17, 117–119.
Carreras, J., Druguet, E., Griera, A., 2005. Shear zone-related folds. Journal of Structural Geology 27, 1229–1251.
Cosgrove, J.W., 1976. The formation of crenulation cleavage. Journal of the Geological Society 132, 155–178.

De Sitter, L.U., 1956. Structural Geology. McGraw-Hill, New York.
Evins, P.M., 2005. A 3D study of aligned porphyroblast inclusion trails across shear zones and folds. Journal of Structural Geology 27, 1300–1314.
Fay, B., Bell, T.H., Hobbs, B.E., 2008. Porphyroblast rotation versus nonrotation: conflict resolution! Geology 36, 307–310.
Fay, C., Bell, T.H., Hobbs, B.E., 2009. Porphyroblast rotation versus nonrotation: conflict resolution!: Reply. Geology 37, p. e188.
Forde, A., Bell, T.H., 1993. The rotation of garnet porphyroblasts around a single fold in the Lukmanier Pass, Central Alps: discussion. Journal of Structural Geology 15, 1365–1368.
Fowler, T.J., Winsor, C.N., 1996. Evolution of chevron folds by profile shape changes: comparison between multilayer deformation experiments and folds of the Bendigo-Castlemaine goldfields, Australia. Tectonophysics 258, 125–150.
Gray, D.R., Durney, D.W., 1979. Investigations on the mechanical significance of crenulation cleavage. Tectonophysics 58, 35–79.
Hayward, N., 1992. Microstructural analysis of the classical spiral garnet porphyroblasts of south-east Vermont: evidence for non-rotation. Journal of Metamorphic Geology 10, 567–587.
Hobbs, B.E., Means, W.D., Williams, P.F., 1982. The relationship between foliation and strain: an experimental investigation. Journal of Structural Geology 4, 411–428.
Hudleston, P., 1999. Strain compatibility and shear zones: is there a problem? Journal of Structural Geology 21, 923–932.
Johnson, S.E., 1990. Lack of porphyroblast rotation in the Otago Schists, South Island, New Zealand: implications for crenulation cleavage development, folding and deformation partitioning. Journal of Metamorphic Geology 8, 13–30.
Jung, W.S., Ree, J.H., Park, Y., 1999. Non-rotation of garnet porphyroblasts and 3-D inclusion trail data: an example from the Imjingang belt, South Korea. Tectonophysics 307, 381–395.
Kraus, J., Williams, P.F., 1998. Relationship between foliation development, porphyroblast growth and large-scale folding in a metaturbidite suite, Snow Lake, Canada. Journal of Structural Geology 20, 61–76.
Means, W.D., 1982. An unfamiliar Mohr circle construction for finite strain. Tectonophysics 89, T1–T6.
Passchier, C.W., Trouw, R.A.J., 2005. Microtectonics, second ed.. Springer, 366 pp.
Passchier, C.W., 1990. Reconstruction of deformation and flow parameters from deformed vein sets. Tectonophysics 180, 185–199.
Paterson, M.S., Weiss, L.E., 1966. Experimental folding in rocks. Nature 195, 1046–1048.
Price, N.J., Cosgrove, J.W., 1991. Analysis of Geological Structures. Cambridge University Press, 502 pp.
Ramsay, J.G., Huber, M.I., 1987. Folds and Fractures. In: Techniques of Modern Structural Geology, vol. 2. Academic Press, 391 pp.
Ramsay, J.G., 1967. Folding and Fracturing of Rocks. McGraw-Hill, 568 pp.
Rich, B.H., 2006. Permian bulk shortening in the Narragansett Basin of southeastern New England, USA. Journal of Structural Geology 28, 682–694.
Sayab, M., 2005. Microstructural evidence for N–S shortening in the Mount Isa Inlier (NW Queensland, Australia): the preservation of early W–E-trending foliations in porphyroblasts revealed by independent 3D measurement techniques. Journal of Structural Geology 27, 1445–1468.
Sayab, M., 2009. Tectonic significance of structural successions preserved within low-strain pods: implications for thin- to thick-skinned tectonics vs. multiple near-orthogonal folding events in the Palaeo-Mesoproterozoic Mount Isa Inlier (NE Australia). Precambrian Research 175, 169–186.
Siddans, A.W.B., 1972. Slaty cleavage – a review of research since 1815. Earth Science Reviews 8, 205–232.
Stewart, L.K., 1997. Crenulation cleavage development by partitioning of deformation into zones of progressive shearing (combined shearing, shortening and volume loss) and progressive shortening (no volume loss): quantification of solution shortening and intermicrolithon-movement. Tectonophysics 281, 125–140.
Stewart, K.G., Alvarez, W., 1991. Mobile-hinge kinking in layered rocks and models. Journal of Structural Geology 13, 243–259.
Timms, N.E., 2003. Garnet porphyroblast timing and behaviour during fold evolution: implications from a 3-D geometric analysis of a hand-sample scale fold in a schist. Journal of Metamorphic Geology 21, 853–873.
Tobisch, O.T., Paterson, S.R., 1988. Analysis and interpretation of composite foliations in areas of progressive deformation. Journal of Structural Geology 10, 745–754.
Vernon, R.H., 2000. Beneath Our Feet: The Rocks of Planet Earth. Cambridge University Press, 216 pp.
Visser, P., Mancktelow, N.S., 1992. The rotation of garnet porphyroblasts around a single fold, Lukmanier Pass, Central Alps. Journal of Structural Geology 14, 1193–1202.
Williams, P.F., 1990. Differentiated layering in metamorphic rocks. Earth Science Reviews 29, 267–281.
Yeh, M.W., 2007. Deformation sequence of Baltimore gneiss domes, USA, assessed from porphyroblast Foliation Intersection Axes. Journal of Structural Geology 29, 881–897.